e-palli

AMERICAN JOURNAL OF
ENERGY AND NATURAL RESOURCES (AJENR)

ISSN: 2835-9186 (ONLINE)

VOLUME 2 ISSUE 1 (2023)

American Journal of Energy and Natural Resources (AJENR)

Volume 2 Issue 1, Year 2023
ISSN: 2835-9186 (Online)
DOI: https://doi.org/10.54536/ajenr.v2i1.1219
https://journals.e-palli.com/home/index.php/ajenr

Selection of a Suitable Material by a Multi-Criteria Decision Aid Method (MCDM) for the Manufacture of the Buckets of a Micro Pelton Turbine

Uwayezu Emmanuel[1*], Hakizabera Olivier[2], Hirwa Gloria[3], Nkubito Muhayeyezu Jean Olivier[4]

Article Information

Received: January 18, 2023

Accepted: February 02, 2023

Published: February 06, 2023

Keywords

Evacuated Tube Solar Collector, Inertia of Water, Optimal flow control

ABSTRACT

This article aims to investigate the effect of inertia on the outlet temperature of an evacuated tube solar collector. The experiments were conducted during a 24h period in Minquin County (latitude 38034'N, Longitude 10303'E). An analysis was made to determine whether the evacuated tube solar collectors' fluid thermal inertia impacts the water storage tank temperature. The results showed differences between the useful energy delivered to the water storage tank in the case with mass flow rate adjusted depending on the incident solar radiation for the entire two days in which experiments were conducted. Two days of cloud and sunshine were considered. An indirect optimal control technique refers to the impacts of the inertia of water on the outlet collector temperature, the on/off control of the pump, and the useful heat gain from the storage tank. During days with clear sky, the average solar radiation, mass flow rate, outlet, and tank temperature were 640.02W/m^2, 0.06kg/s, 29^{0}C, and 44.24^{0}C, respectively. For cloudy day was 449W/m^2, 0.02kg/s, 27^{0}C and 42^{0}C respectively. The control system is provided to run the heating circulating pump after rest for several minutes to facilitate the exhaust system, then continues to run for a cycle. The $D_{TP,ON}$ and $D_{TP,OFF}$ range from 3^{0}C to 10^{0}C and from 0.2^{0}C to 1.5^{0}C, respectively.

INTRODUCTION

China has become the world's most extensive solar water heating system for production and applications. Moreover, automated control technology has advanced and improved significantly, making it feasible to handle even complex systems. Early approaches to energy gain maximization through mass flow rate control are reported in Refs. (Kovarik et al., 1976) and (Bejan et al., 1982). More recently, little work has been done to investigate the dynamic characteristics that affect the performance of the entire thermal systems, including heating, air conditioning, and control systems. Much research on the collector's thermal properties is concentrated on the steady-state or quasi-steady-state process [John et al.,1991, Han Zongwei et al., 2008]. For instance, the minimum cost per unit of energy transferred was considered (Horel et al.,1978), while in (Hollands et al., 1992), the amount of collected energy was maximized. Different optimal strategies were found when the exergy gain was analyzed (Bejan, 1982). More advanced approaches assume the controlled variable is the energy gain (to be maximized), the amount of collected energy (to be maximized), and the exergy gain (to be maximized) (Kovarik et al., 1976, Horel et al., 1978, Bejan et al., 1982, Hollands et al., 1992).

The optimal flow rate control in a solar collector under simplified weather conditions (assumed as sinusoidal time functions) was studied by (Saltiel et al., 1985). The optimal control of a closed-loop system based on a realistic solar collector model was analyzed using a sizeable meteorological database (Badescu, 2008). Two empirical control strategies have been proposed by (Furbo et al., 1996) for a solar domestic hot water system. The second method from (Furbo et al., 1996) has been slightly changed recently in (Nhut et al., 2013), where simulations have been performed under South Korean latitudes and climates over a single spring day. In this paper, the heat-balanced equation for solving the collector temperature in the unsteady state was theoretically and experimentally developed, and a detailed study of the influence of water inertia on the solar heating system was presented. The main focus is on the all-glass evacuated tube solar collector and from the angle of the entire solar water heating system (including the control system), thoroughly studying the effect of water inertia on the outlet collector water temperature, the on/off control of pump and the heat gain.

METHODOLOGY

The energy-balanced equation can describe the heat transfer process of solar collectors. In the steady state, the incident radiation on the collector surface is equal to the sum of heat and several different loss terms, as is evident from the energy balance of the absorber of a solar thermal collector, which is given by the following expression:

$$\frac{Q}{A_c} = \frac{mC_p(T_o - T_i)}{A_c} = F_R[(\tau\alpha)G_T - U_L(T_i - T_a)] \qquad (1)$$

The collector efficiency calculate by integrating hour-step efficiency and is expressed as:

$$\eta = \frac{mC_p(T_o - T_i)}{A_c * G_T} = F_R(\tau\alpha) - F_R U_L \frac{(T_i - T_a)}{G_T} \qquad (2)$$

Where:

- Ac is Evacuated tube solar collector absorber area, m^2
- GT is the global intensity of solar radiation, W/m^2
- T_0 is outlet temperature, ^{0}C

[1] College of Mechanical and Vehicle Engineering, Taiyuan University of Technology, China
[2] China Western Research Center of Energy & Environment, Gansu Key Laboratory of Complementary Energy System of Biomass and Solar energy, China.
[3] School of Architecture and Design, Beijing Jiaotong University, China
[4] Mechanical Engineering Department, RP (IPRC Kigali), Rwanda
[*] Corresponding author's email: Kyrieguy11@gmail.com

- T_i is inlet temperature, ^{0}C
- Ta is ambient temperature, ^{0}C
- Ts is tank temperature, ^{0}C
- Q is Useful energy gain, W
- m is the mass flow rate of fluid through the collector, kg/s
- C_p is the Heat capacity of water, kJ/kg^{0}C
- η is clean collector efficiency
- Fr is The collector heat removal factor
- UL is the heat coefficient between the water tank and the ambient temperature
- T is the transmission coefficient of glazing
- τ α is the Absorptance-transmittance product

The condition of the controller to turn the pumps is when the value of solar energy delivered to the load exceeds the value of the energy needed to operate the pump [16]. Control systems are often used when the mass flow rate has two allowable values: maximum and zero. A solar radiant floor heating system was established to analyze the dynamic performance. It consists of a solar water heating system (including a pump control system, and the radiant floor heating system.

Pump P starts when the exit temperature from the solar collectors exceeds $D_{TP, ON}$ the temperature Ts in the water storage tank. The pump P stops if To-Ts < $D_{TP, OFF}$

$$Q_u = \begin{cases} 0 & (Pump\ P\ does\ not\ operate) \\ \frac{mC_p(T_o - T_i)}{A_c} = F_R[(\tau\alpha)G_T - U_L(T_i - T_a)] & (Pump\ P\ operate) \end{cases} \quad (3)$$

$$Q_u = \begin{cases} To - Ts < DT_{P,OFF} & (Pump\ P\ does\ not\ operate) \\ To - Ts > DT_{P,ON} & (Pump\ P\ operate) \end{cases} \quad (4)$$

System Description

The schematic of the experiment is shown in Figure. 1, and the technical specification is in table 1. The Evacuated Tube Solar Collector was experimentally investigated at Minquin County (latitude 38034'N, Longitude 10303'E). The typical control system has four heat coils with platinum resistance temperature sensors (pt100, manufactured by Beijing Sailing Technology Co., Ltd., with a precision of ±0.1 °C) mounted on the ambient, inlet, outlet, and tank of the collector. The flow rate of hot water with an LWGY-15 turbine flow meter (manufactured by Shanghai Huaman Industrial Co., Ltd., with a precision of ±0.45%). The total solar radiation was recorded by Pyranometers (Kipp & Zonen CM11). Each measuring instrument connect to the computer via interfaces and is automatically scanned at 10s intervals and recorded by Agilent 349702

Meteorological and Actinometric Data

The weather data was experimentally investigated at Minchin, China. The data was chosen for Sunny and Cloudy day. The performance of experiments was conducted for a whole day. Measurements were recorded every 10 seconds. The data obtained from the tests in the system are based on 16 and 27th December, 2014. Sunny day maximum value of ambient temperature and Solar radiation (Figure.1 and 2) was 14.37^{0}C and 945.6W/m^2, respectively, while for the cloudy day was 8.1^{0}C and 861.2 W/m^2, respectively.

Table 1: Technical specifications

Absorbing coating	Absorptivity [-] 0.94 Emissivity [-] 0.06
Outer glass envelope and absorber glass tube	Outer diameter of glass envelope [m] 0.058 Outer diameter of absorber tube [m] 0.047 Glass tube length [m] 1.56 Aperture width [m] 0.1105 Thickness of glass [m] 0.0016 Thermal conductivity of glass [W/(m K)] 1.2 Transmittance of glass [-] 0.92
Aluminum fin	Thickness [m] 0.0008 Thermal conductivity [W/(m K)] 220
Copper U-tube	Outer diameter [m] 0.0063 Thickness [m] 0.0005 Thermal conductivity [W/(m K)] 370
Header section	Outer diameter [m] 0.0063 Thickness [m] 0.0005 Thermal conductivity [W/(m K)] 370
Number of glass tubes	30

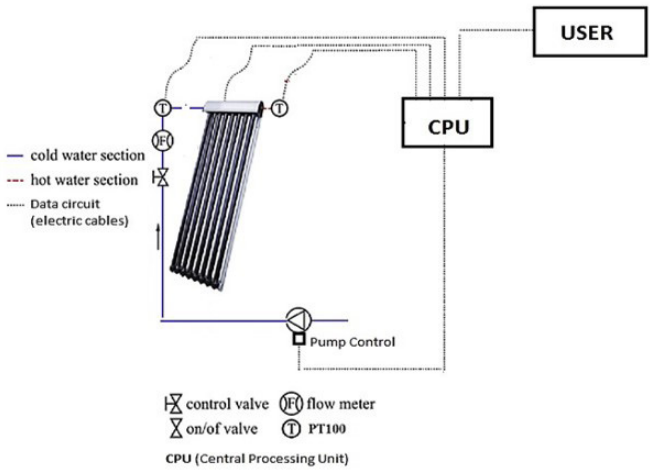

Figure 1: Experiment Control system

RESULTS

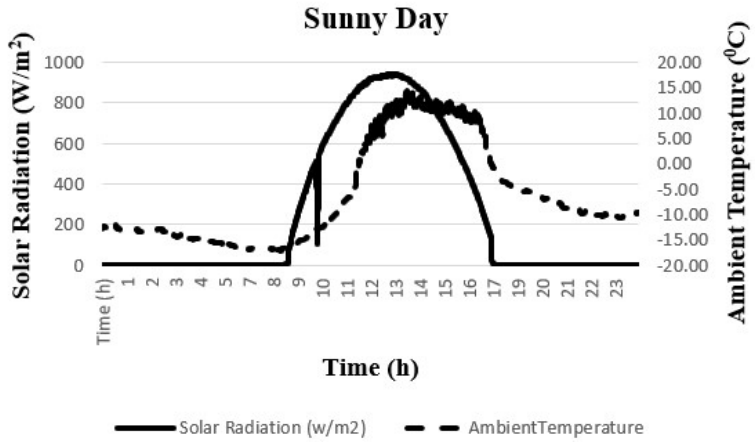

Figure 2: Solar Radiation on 16th December 2014

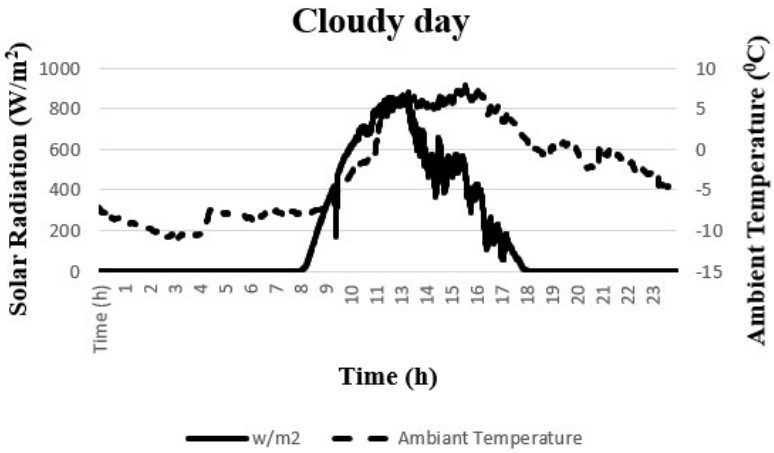

Figure 3: Solar Radiation on 27th December 2014

Table 2: Experiment results for Sunny day

	Solar Radiation (w/m²)	Outlet Temperature (⁰C)	Inlet Temperature (⁰C)	Tank temperature (⁰C)	Ambient Temperature (⁰C)	Mass Flowrate (kg/s)
min	0.11	11.00	13.66	35.81	-17.17	0.00
max	945.65	65.77	60.10	58.84	14.37	0.30
average	640.02	29.25	32.97	44.24	-6.43	0.06

Table 3: Experiment results for Sunny day

	Solar Radiation (w/m^2)	Outlet Temperature (^0C)	Inlet Temperature (^0C)	Tank temperature (^0C)	Ambient Temperature (^0C)	Mass Flowrate (kg/s)
min	0.11	11.00	13.66	35.81	-17.17	0.00
max	945.65	65.77	60.10	58.84	14.37	0.30
average	640.02	29.25	32.97	44.24	-6.43	0.06

DISCUSSIONS

After the outdoor temperature and the incident solar radiation have been specified, two sets of conditions of thermal inertia have been investigated for cloudy and Sunny days. The hourly variation of inlet, outlet (inertia–considered models), and Tank temperature. In literature(Knudsen, S, 2002), the control strategy and operation are as follows. Figure 4 (a,b) shows Pump P starts when the exit temperature from the solar collectors, To, exceeds by $D_{TP,ON}$ the temperature Ts in the water storage tank. The pump P stops if To -Ts < $D_{TP,OFF}$. Usual values of $D_{TP,ON}$ and $D_{TP,OFF}$ range from 3^0C to 10^0C and from 0.2^0C to 1.5^0C, respectively.

During the night, the pump at the collector side turned off, and the water in the collector was in thermal equilibrium. For a sunny day, the water temperature increased sharply without considering the inertia of the water, causing the pump to switch on at 17h00 and transfer heat to the storage tank, shown in Figure 4 (a). The difference between Tank and outlet temperature ($D_{TP,ON}$>3 ^0C). After 17:00, the solar radiation was unable to provide sufficient heat, which resulted in shutting down the pump at 23h00. The outlet and Tank temperature of the inertia model fell rapidly, then reduced slowly to its minimum. The difference between the Tank and outlet temperature ($D_{TP,OF}$F<0.2^0C) decreased until the night (23h00) turned, and the water in the collector was in thermal equilibrium. Sunshine duration was 9 hours and 21 Minutes, as shown in Figure 2. The average solar radiation intensity, mass flow rate, and ambient temperature were $248.1W/m^2$, 0.06kg/s, and -6.4℃, respectively (table 2). The data analysis based on equation (3) provides heat to that day of 10311.96 kW.

For a cloudy day, the pump switched on at 17h00 and transferred heat to the storage tank, shown in Figure 5 (b). Because of that day, the solar radiation was low to provide sufficient heat, the pump shut down the pump at 21h03, and the water in the collector was in thermal equilibrium. Solar heating is shown on a cloudy day for a heating cycle and a return flow temperature curve

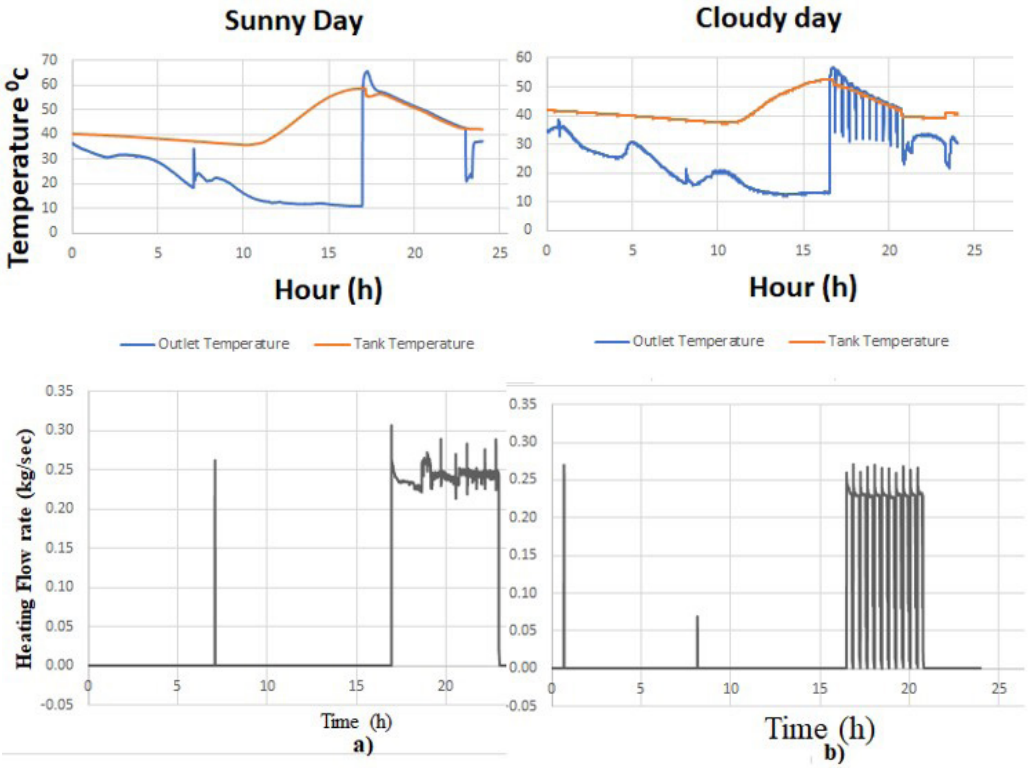

Figure 4: Optimal control of the inertia on 16 and 27th December 2014 Optimal control of the inertia on 16 and 27th December 2014

over time. The control system is provided to run the heating circulating pump and rest for several minutes to facilitate the exhaust system, then continues to run for a cycle. Sunshine duration was 9 hours 34 Minutes, as shown in Figure 3, the average solar radiation intensity and ambient temperature were 449W/m^2, 0.02kg/s, and -3℃, respectively (table 3). The heat provided that day was 7641.192 kW.

CONCLUSION

Conventional models should have considered the influence of the inertia of water in the collectors, which would result in incomprehensive recognition of the dynamic characteristic of collectors, thus affecting the objective assessment of the entire thermal system. For all-glass evacuated tube solar collectors, increasing pump turn-on time, the inertia of water decrease, and lost heat gain from the storage tank, whereas the pump will be on/off more frequently. For a sunny day, the difference between Tank and outlet temperature ($D_{TP,ON}$ >3^{0}C) and ($D_{TP,OFF}$ <0.2^{0}C). After 17:00, the solar radiation was unable to provide sufficient heat, which resulted in shutting down the pump at 23h00. The outlet and Tank temperature of the inertia model fell rapidly, then reduced slowly to its minimum. For cloudy, the difference between $D_{TP,ON}$ and $D_{TP,OFF}$ is the same. But that day, the solar radiation was low to provide sufficient heat, the pump shut down the pump at 21h03, and the water in the collector was in thermal equilibrium.

Reducing water inertia will increase pump turn-on time and heat gain depending on meteoritical conditions. This research will help relevant experts to evaluate the solar energy system more accurately, and the existing will improve solar energy, simulation models.

REFERENCES

Badescu, V. (2008). Optimal control of flow in solar collector systems with fully mixed water storage tanks. Energy Convers. *Manage., 49*(2), 169–184.

Beckman, W.A., Thornton, J., Long, S., & Wood, B.D. (1994). Control problems in solar domestic hot water systems. *Solar Energy, 53*(3), 233–6.

Bejan, A. (1982). Extraction of exergy from solar collectors under time varying conditions. *Int. J. Heat Fluid Flow, 3*(2), 67–72. doi.org/10.1016/j.apm.2016.12.033

Bejan, A., & Schultz, W. (1982). Optimum flow-rate history for cooldown and energy storage processes. Int. J. *Heat Mass Transfer, 25*(8), 1087–92. doi.org/10.1016/0142-727X(82)90002-9

Bejan, A., and Schultz, W. (1982). Optimum flow-rate history for cooldown and energy storage processes. *Int. J. Heat Mass Transfer, 25*(8), 1087–1092.

Furbo, S., and Shah, L. J. (1996). Optimum solar collector fluid flow rates. Proc., EuroSun, DGS Sonnenenergie Verlags, DGS Sonnenenergie Verlags, Munich, 189–193.

Han Zongwei, Zheng Maoyu. Experimental Research on Solar Assisted Ground Source Heat Pump Heating System with a Latent Heat Storage Tank in Severe Cold Area. *Acta Energiae Solaris Sinica, 29*(5), 574-580, 2008. doi.org/10.17577/ijertv3Is040400.

Hollands, K. G. T., and Brunger, A. P. (1992). Optimum flow rates in solar water heating systems with a counterflow exchanger. *Solar Energy, 48*(1), 15–19.

Horel, J. D., and De Winter, F. (1978). Investigations of methods to transfer heat from solar liquid-heating collectors to heat storage tanks. Final Rep. on U.S. Dept. of Energy Contract E(4)1238, Altas Corporation, Santa Cruz, CA.

John A. Duffie. Solar Engineering of Thermal Processes. Culinary & Hospitality Industry Publications Services, John Wiley & Sons, Incorporated, New York, 1991, 20-22

Knudsen, S. (2002). Consumers' influence on the thermal performance of small SDHW systems. *Solar Energy, 73*(1), 33–42. doi.org/10.1016/S0038-092X(02)00018-X

Kovarik, M., and Lesse, P. F. (1976). Optimal control of flow in low temperature solar heat collectors. *Solar Energy, 18*(5), 431–435. doi.org/10.1016/0038-092X(76)90009-8

Nhut, L. M., and Park, Y. C. (2013). A study on automatic optimal operation of a pump for solar domestic hot water system. *Solar Energy, 98,* 448–457.

Saltiel, C., and Sokolov, M. (1985). Optimal control of a multicomponent solar collector system. *Solar Energy, 34*(6), 463–473. doi.org/10.1016/0038-092X(85)90020-9

$$r_{ij} = X_{ij} \Big/ \sqrt{\sum_{i=1}^{i=m} x_{ij}^2} \quad \text{Where } i=1, 2, 3, \ldots, m \text{ and } j=1, 2, 3, \ldots, n$$

$$S_j = \sum_{i=1}^{n} w_i \left(f_i^* - f_{ij}\right)/(f_i^* - f_i^-) \qquad 17$$

$$R_j = max_i \left[(f_i^* - f_{ij})/(f_i^* - f_i^-)\right] \qquad 18$$

$$Q_j = \vartheta \frac{(S_j - S^*)}{(S^- - S^*)} + (1-\vartheta)\frac{(R_j - R^*)}{(R^- - R^*)} \qquad 19$$

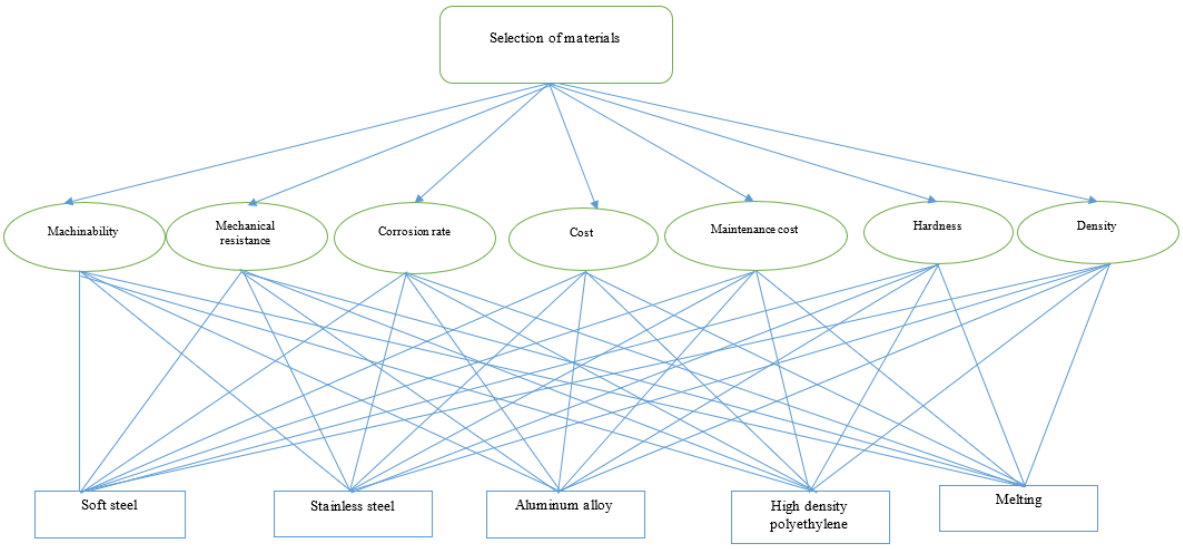

Figure 2 : The decision-making hierarchy by the AHP.

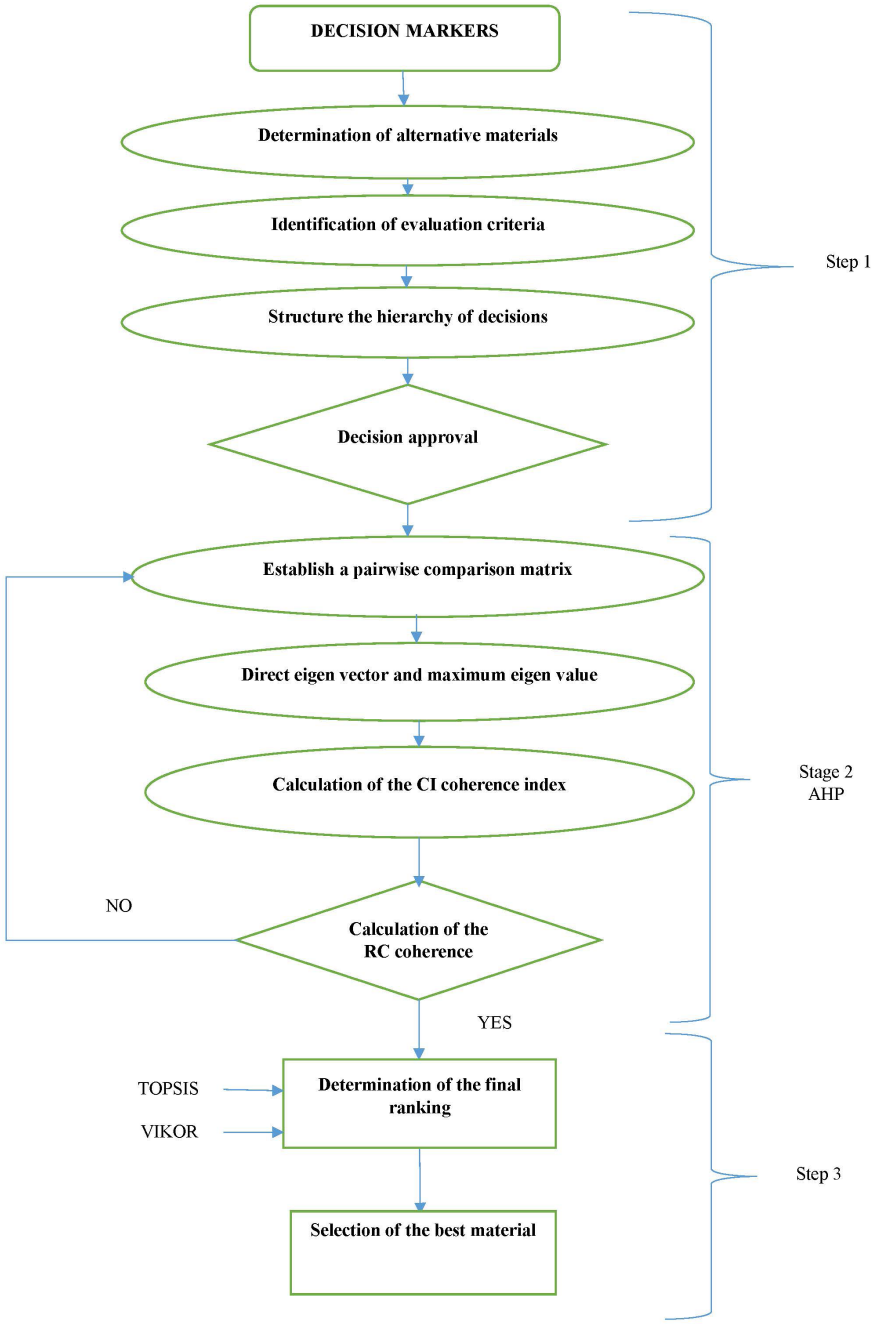

Figure 3 : Schematic flow chart of developed methodology for optimal material selection

Table 3: The pairwise comparison matrix developed using the AHP method for the seven (7) criteria.

	Machinability	Corrosion resistance	Density (kg/cm3)	Tensile strength Rm (Mpa)	Hardness	Cost (€ / kilo)	Maintenance cost
M	1.0000	7.0000	3.0000	4.0000	3.0000	4.0000	2.0000
UTS	0.1429	1.0000	0.3333	0.5000	0.3333	0.2000	0.5000
D	0.3333	3.0000	1.0000	3.0000	3.0000	2.0000	5.0000
RC	0.2500	2.0000	0.3333	1.0000	0.3333	0.3333	0.5000
H	0.3333	3.0000	0.3333	3.0000	1.0000	3.0000	3.0000
RC	0.2500	5.0000	0.5000	3.0000	0.3333	1.0000	2.0000
CM	0.5000	2.0000	0.2000	2.0000	0.3333	0.5000	1.0000
TOTAL	2.8095	23.0000	5.7000	16.5000	8.3333	11.0333	14.0000

We used equation (2) for matrix normalization.

Table 4: Normalization of the expanded pairwise comparison matrix.

Criteres	M	Uts	D	Cr	H	Cr	Cm
M	0,32777357	0,27694945	0,64489173	0,22911482	0,46952812	0,48537338	0,16513379
UTS	0,0468	0,0396	0,0717	0,0286	0,0522	0,0243	0,0413
D	0,1093	0,1187	0,2150	0,1718	0,4695	0,0589	0,4128
CR	0,0819	0,07912842	0,0717	0,0573	0,0522	0,0404	0,0413
H	0,1093	0,11869262	0,0717	0,1718	0,1565	0,3640	0,2477
CR	0,0819	0,19782104	0,1075	0,1718	0,0522	0,1213	0,1651
CM	0,1639	0,07912842	0,0430	0,1146	0,0522	0,0607	0,0826
TOTAL	0,9209	0,9100	1,2253	0,9451	1,3042	1,1550	1,1559

To determine the consistency analysis of the pairwise comparison matrix, equations (3), (5), and (6) are used. Thus Table 5 presents the result obtained with the AHP method.

Table 5: The result obtained by the AHP method.

Criteria	Weight	λ_max	CI	CR
M	0.32777357	7.54269427	0.09044904	0.06699929
UTS	0.03956421			
L	0.21496391			
D	0.0572787			
VS	0.15650937			
RC	0.12134335			
CM	0.08256689			

After determining the weight of the criteria with the AHP, we will apply the TOPSIS technique to rank the selected alternatives. Thus Table 6 shows the vector matrix.

Table 6: Vector matrix of chosen materials

Materials/ Alternatives		Properties					
	Machinability	Corrosion resistance	Density (kg/cm3)	Tensile strength (Mpa)	Hardness	Cost (€/kilo)	Maintenance cost
Soft steel	3	1	7.85	400	5	1.25	4
Stainless steel	4	4	7.7	720	4	1.5	3
HDPE high density polyethylene	5	5	0.965	6	2	1.67	2
Melting	3	2	7.2	350	4	0.9	4
Aluminum alloy	4	5	2.7	80	4	2.48	2

Table 7 : The standardized decision matrix with criteria and alternatives.

Criteria / Alternatives	Machinability	Corrosion resistance	Density	Tensile strength	Hardness	Cost (price)	Maintenance cost
Soft steel	0.043478261	0.01408451	0.06171324	0.000617536	0.0877193	0.09434461	0.10810811
Stainless steel	0.057971014	0.05633803	0.06053401	0.001111564	0.07017544	0.11321353	0.08108108
HDPE	0.072463768	0.07042254	0.0075864	9.26303E-06	0.03508772	0.12604439	0.05405405
Melting	0.043478261	0.02816901	0.05660323	0.000540344	0.07017544	0.06792812	0.10810811
Aluminum alloy	0.057971014	0.07042254	0.02122621	0.000123507	0.07017544	0.1871797	0.05405405

Table 8 : The weighted normalized decision matrix with criteria and alternatives

Criteria / Alternatives	Machinability	Corrosion resistance	Density	Tensile strength	Hardness	Cost (price)	Maintenance cost
Soft steel	0.014251025	0.00055724	0.01326612	3.53716E-05	0.01372889	0.01144809	0.00892615
Stainless steel	0.019001366	0.00222897	0.01301263	6.36689E-05	0.01098311	0.01373771	0.00669461
HDPE	0.023751708	0.00278621	0.0016308	5.30575E-07	0.00549156	0.01529465	0.00446308
Melting	0.014251025	0.00111448	0.01216765	3.09502E-05	0.01098311	0.00824262	0.00892615
Aluminum alloy	0.019001366	0.00278621	0.00456287	7.07433E-06	0.01098311	0.02271301	0.00446308
Weight	0.327773567	0.03956421	0.21496391	0.057278704	0.15650937	0.12134335	0.08256689

Table 9 : The calculation of the best ideal value and the worst ideal value

V+	0.023751708	0.00278621	0.0016308	6.36689E-05	0.00549156	0.02271301	0.00892615
V-	0.014251025	0.00055724	0.01326612	5.30575E-07	0.01372889	0.00824262	0.00446308

Table 10: The Euclidean distance () best ideal () worst ideal and the performance score used for rankingS_i^+ S_i^-

Alternatives	S_i^+	S_i^-	Pi	Rank
Soft steel	0.020624374	0.00549502	0.21038089	4
Stainless steel	0.016374223	0.00825492	0.33516871	3
HDPE	0.008657663	0.01866003	0.68307485	1
Melting	0.021062601	0.00538297	0.20354916	5
Aluminum alloy	0.009013445	0.01789447	0.66502624	2

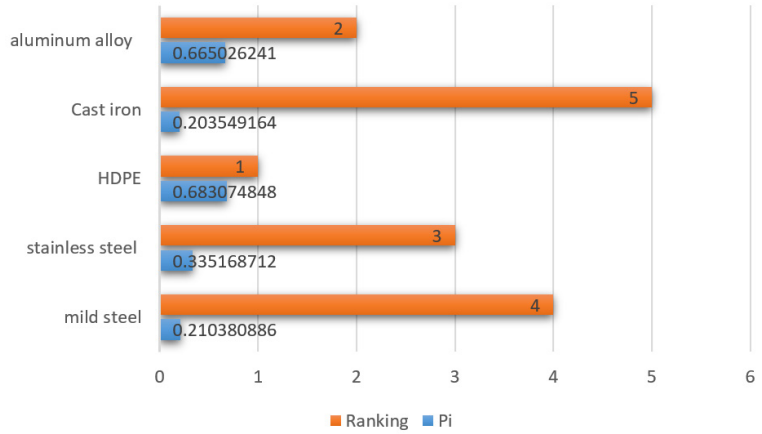

Figure 4: Classification diagram TOPSIS method

Table 11: The standardized decision matrix

Criteria	Machinability	Corrosion resistance	Density	Tensile strength	Hardness	Cost (price)	Maintenance cost
Soft steel	0.04347826	0.01408451	0.06171324	0.00061754	0.0877193	0.09434461	0.10810811
Stainless steel	0.05797101	0.05633803	0.06053401	0.00111156	0.07017544	0.11321353	0.08108108
HDPE	0.07246377	0.07042254	0.0075864	9,263E-06	0.03508772	0.12604439	0.05405405
Melting	0.04347826	0.02816901	0.05660323	0.00054034	0.07017544	0.06792812	0.10810811
Aluminum alloy	0.05797101	0.07042254	0.02122621	0.00012351	0.07017544	0.1871797	0.05405405

The best and worst values for each criterion are calculated using Equation 17 and the resulting values are tabulated in Table 12.

Table 12: The best and the worst values of each criterion

X+	Best	5.0000	5.0000	7.8500	720.0000	5.0000	2.4800	4.0000
X-	worth	3.0000	1.0000	0.9650	6.0000	2.0000	0.9000	2.0000

Table 13: Result of the classification by the VIKOR method

Criteria	Machi -nability	Corrosion resistance	Density	Tensile strength	Hard-ness	Cost (price)	Mainte-nance cost	Si	Ri	Qi	rank
Soft steel	0.81230841	0.04931595	0.24316639	0.05775999	0.25627266	0.18321735	0.16067071	1.76271144	0.81230841	0.52072945	4
Stain lesssteel	0.80993323	0.04889802	0.2432032	0.05775999	0.25718791	0.18176822	0.16178648	1.76053706	0.80993323	0.26275352	3
HDPE	0.80755806	0.04875871	0.24485634	0.05775999	0.25901843	0.18078282	0.16290225	1.7616366	0.80755806	0.01678676	1
Melting	0.81230841	0.04917664	0.37101953	0.05775999	0.25718791	0.18524612	0.16067071	1.89336931	0.81230841	1	5
Aluminum alloy	0.80993323	0.04875871	0.24443048	0.05775999	0.25718791	0.17608765	0.16290225	1.75706022	0.80993323	0.25	2
							S*,R*	1.75706022	0.80755806		
							S-,R-	1.89336931	0.81230841		

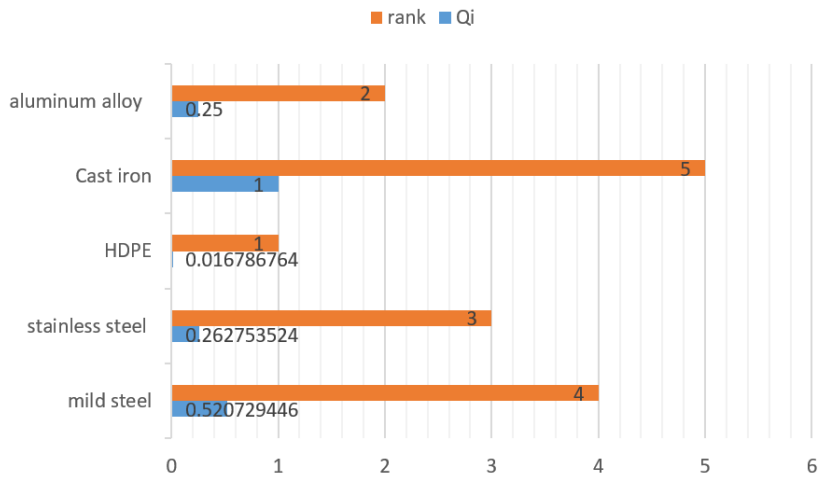

Figure 5 : Classification diagram VIKOR method